Published in final edited form as:
Bone. 2010 January ; 46(1): 129. doi:10.1016/j.bone.2009.09.025.

Pathway-based Genome-Wide Association Analysis Identified the Importance of EphrinA-EphR pathway for Femoral Neck Bone Geometry

Yuan Chen[1,*], **Dong-Hai Xiong**[2,*], **Yan-Fang Guo**[1], **Feng Pan**[1], **Qi Zhou**[1], **Feng Zhang**[1], and **Hong-Wen Deng**[1,2,3]

[1] The Key Laboratory of Biomedical Information Engineering of Ministry of Education and Institute of Molecular Genetics, School of Life Science and Technology, Xi'an Jiaotong University, Xi'an, Shaanxi 710049, P. R. China

[2] Departments of Orthopedic Surgery and Basic Medical Sciences, University of Missouri - Kansas City, Kansas City, MO 64108, USA

[3] College of Life Sciences and Engineering, Beijing Jiaotong University, Beijing 100044, P. R. China

Abstract

Femoral neck (FN) bone geometry is an important predictor of bone strength with high heritability. Previous studies have revealed certain candidate genes for FN bone geometry. However, the majority of the underlying genetic factors remain to be discovered. In this study, pathway-based genome-wide association analysis was performed to explore the joint effects of genes within biological pathways on FN bone geometry variations in a cohort of 1,000 unrelated U.S. whites. Nominal significant associations (nominal p value < 0.05) were observed between 76 pathways and a key FN bone geometry variable - section modulus (Z), biomechanically indicative of bone strength subject to bending. Among them, EphrinA-EphR pathway was most significantly associated with FN Z even after multiple testing adjustments (p_{FWER} value = 0.035). The association of EphrinA-EphR pathway with FN Z was also observed in an independent sample from Framingham Osteoporosis Study. Overall, these results suggest the significant genetic contribution of EphrinA-EphR pathway to femoral neck bone geometry.

Keywords

Bone strength; Femoral neck bone geometry; Genetic factor; Pathway-based genome-wide association analysis; EphrinA-EphR pathway

Corresponding author: Hong-Wen Deng, Ph. D. The Key Laboratory of Biomedical Information Engineering of Ministry of Education and Institute of Molecular Genetics, School of Life Science and Technology, Xi'an Jiaotong University, Xi'an 710049, P. R. China, Tel: 816-235-5354, Fax: 816-235-6517, dengh@umkc.edu.
*Equal contribution

INTRODUCTION

Hip fracture occurs when the load applied to hip bone exceeds its mechanical strength. The mortality and morbidity associated with hip fracture become an ever-increasing threat to the public health [1]. Femoral neck (FN) bone geometry, an important predictor of bone strength, is under strong genetic control with heritability ranging from 30–70% [2;3]. To date, some studies have been carried out to identify the genetic basis of FN bone geometry, with certain progresses being made [4–6]. However, the majority of FN bone geometry candidate genes are still largely unknown, leaving a considerable gap in knowledge.

Recently, a pathway-based approach was proposed to further interpret genome-wide association (GWA) data at the level of gene sets [7]. Generally speaking, it is a pathway-driven gene set enrichment analysis, which focuses on groups of genes [i.e. genes sharing a biochemical or cellular function, chromosomal location or regulation, or Gene Ontology (GO) category] that make modest contributions to disease risk, rather than a few single nucleotide polymorphisms (SNPs) and/or genes with strong evidence of association. The method starts with gene ranking based on its degree of association with the studied phenotype to generate a gene list, then uses a statistic enrichment score (*ES)* to determine whether members of a given gene set tend to be concentrated at the top (or bottom) of the list, i.e. the gene set is related to the phenotype. The significance of *ES* is assessed by comparing it with the set of score obtained by 1,000 re-sampling runs, adjusting for variation in gene size and controlling for family-wise error rate (*FWER)*. Through application to two Parkinson diseases (PD) and one amyotrophic lateral sclerosis (AMD) GWA data sets, this approach was proven to be powerful in the exploration of disease-susceptibility mechanism [7].

To identify the potential pathway underlying FN bone geometry variation, we employed this approach to analyze the GWA data from a cohort of 1,000 unrelated U.S. whites. We detected an interesting pathway for FN bone geometry – EphrinA-EphR signaling pathway, whose significant relevance to FN bone geometry was verified in an independent sample from Framingham Osteoporosis Study and some of whose gene components have been known to be important for bone. Our findings have important implications regarding the genetic regulation of bone strength and the pathogenesis of hip fracture.

MATERIALS AND METHODS

Subjects and phenotypes

The study was approved by the Institutional Review Board of University of Missouri – Kansas City. Signed informed-consent documents were obtained from all study participants before they entered the study. The basic characteristics of the study subjects are summarized in Table 1.

U.S. whites—Based on our established and expanding genetic repertoire with more than 6,000 subjects, a total of 1,000 unrelated healthy U.S. whites were selected for this study. They were normal healthy subjects defined by a comprehensive suite of exclusion criteria [8]. Briefly, efforts were made to exclude subjects with chronic diseases and conditions that might potentially affect bone metabolism so as to increase the statistical power for detecting bone candidate genes.

Areal bone mineral density (BMD, g/cm^2) and bone size (cm^2) of FN were measured by using dual energy X-ray absorptiometry (DXA) machines (Hologic Inc., Bedford, MA, USA). The machines were calibrated daily. The coefficient of variation (CV) values of the DXA measurements for FN BMD and bone size were 1.87% and 1.97%, respectively. On the basis of FN BMD and FN bone size, hip structural or hip strength analysis (HSA) was applied to

estimate four parameters, which are generally used to describe bone strength in the proximal femur. They are section modulus (Z, in cm^3), an index of bone bending strength; cross-sectional area (CSA, in cm^2), an indicator of bone axial compression strength; cortical thickness (CT, in cm), an estimate of mean cortical thickness; and buckling ratio (BR), an index of bone structural instability. Briefly, the method assumes that: 1) the cross-section of bone within the femoral neck region is a right circular annulus; 2) 60% of the measured bone mass is cortical; 3) the effective BMD in fully mineralized bone tissue is 1.05 g/cm^3. All of these assumptions were substantiated as good approximations [9]. The formulas used to calculate the five parameters are presented below.

$$CSA = \frac{BMD^{*}W}{1.05},$$

where W is the FN periosteal diameter and can be approximated by dividing FN bone size by the width of the region of interest (in Hologic DXA systems, the width of the FN region is standardized at 1.5cm [10]);

$CT = \frac{W - ED}{2}$, where the ED (Endocortical diameter) is calculated by the formula

$$ED = 2\sqrt{\left(\frac{W}{2}\right)^2 - 60\%^{*}\frac{CSA}{\pi}};$$
$$BR = \frac{W/2}{CT};$$
$$Z = \frac{CSMI}{W/2},$$

where the $CSMI$ (Cross-sectional moment inertia) is calculated by the formula

$CSMI = \frac{\pi}{4}\left[\left(\frac{W}{2}\right)^4 - p\left(\frac{ED}{2}\right)^4\right]$, p as trabecular porosity is calculated by the formula

$p = 1 - \left[\frac{1 - 60\%^{*}CSA}{\pi^{*}\left(\frac{ED}{2}\right)^2}\right]$. Details of the phenotype definitions were previous reported [4;11].

Framingham sample—A set of 1,151 unrelated Framingham subjects were chosen from Framingham Osteoporosis study [12]. The participants underwent bone densitometry by DXA with a Lunar DPX-L (Lunar Corp., Madison, WI, USA). Femoral geometry parameters was assessed noninvasively by DXA-based HSA [11;13]. The region assessed was the narrowest width of the femoral neck (NN), which overlaps or is proximal to the standard femoral neck region. FN CSA, and FN Z were measured directly from the mass profiles using a principle first described by Martin and Burr [14]. The CV values for the different variables were previously reported to range from 7.9% (CSA) to 10.4% (BR). Detail descriptions could be found in the corresponding previous reports [12;15].

Genotyping

U.S. whites—Genomic DNA was extracted from whole human blood using a commercial isolation kit (Gentra systems, Minneapolis, MN, USA) following the protocols detailed in the kit. DNA concentration was assessed by a DU530 UV/VIS spectrophotometer (Beckman Coulter, Inc, Fullerton, CA, USA). Before advancing to the hybridization step, the measurements of DNA concentration were double-checked by pico-green analysis that can detect fluorescent signal enhancement of PicoGreen® dsDNA Quantitation Reagent, which

selectively binds to dsDNA [16;17]. Genotyping with Affymetrix mapping 500K array (Affymetrix, Inc., Santa Clara, CA) was performed at the Vanderbilt Microarray Shared Resource at Vanderbilt University Medical Center, Nashville, TN using the standard protocol recommended by the manufacturer (see detailed description in [8]). Genotyping calls were determined with the dynamic model (DM) algorithm [18] as well as with the B-RLMM (Bayesian Robust Linear Model with Mahalanobis Distance Classifier) algorithm, an extention of the RLMM (Robust Linear Model with Mahalanobis Distance Classifier) [19] developed for the Mapping 500K product. DM calls were used for quality control of the genotyping experiment, and unsatisfactory arrays were subjected to re-genotyping. Eventually, 997 subjects (501 males and 496 females) who had at least one array (Nsp or Sty) reaching 93% call rate were retained. BRLMM calls were used for the following pathway-based GWA analyses, where only autosomal SNPs with per-SNP call rates (i.e. call rate for each SNP across all samples) > 95%, Hardy-Weinberg equilibrium (HWE) p values >= 0.001, minor allele frequencies (MAF) >= 5% and the physical distances from genes < 500 kb were evaluated. The distance setting was from the consideration that most enhancers and repressors are < 500 kb away from genes and most LD blocks are < 500 kb.

Framingham sample—Genotype (Affymetrix 500K mapping array plus Affymetrix 50K supplemental array) and phenotype information were downloaded from the dbGaP database (http://www.ncbi.nlm.nih.gov/sites/entrez?db=gap). Data download and usage was authorized by the SHARe data-access committee. Only individuals (469 males and 679 females) with genotypic call rates > 93% and SNPs on a given pathway/gene set with per-SNP call rates > 95%, HWE p value >= 0.001 and MAF >= 5% were included in the following association study.

Pathway/gene sets database construction

We retrieved 260,190 and 380 annotated human pathways from BioCarta pathway database (http://www.biocarta.com/genes), KEGG pathway database (http://www.genome.ad.jp/kegg/pathway.html) and Ambion GeneAssist™ Pathway Atlas (http://www.ambion.com/tools/pathway), respectively. In addition, we downloaded GO annotation files for human genes from the GO website (http://www.geneontology.org) to integrate the GO information into our study. Gene sets were obtained from Level 4 Biological Process and Molecular Function GO terms. Genes whose GO annotations were in level 5 or lower in the GO hierarchy were assigned to their ancestral GO annotations in level 4. In our analysis, we tested only those pathways/gene sets with 10–200 genes included in our GWA data set so as to alleviate the multiple-testing problem by avoiding testing too narrowly- or too broadly- defined functional categories. Overall, 963 pathways/gene sets were constructed by 14,585 genes/312,172 SNPs.

Routine statistical analysis

For raw FN bone geometry in both the U.S. whites and the Framingham sample, we tested their correlations with parameters like age, age^2, sex, age/age^2-by-sex interactions, height and weight. After adjustments for significant (p value < 0.05) terms (age, age^2, sex, height and weight) in each sample, the phenotype data, if not following normal distribution, were further subjected to Box-Cox transformation. General association analyses on individual SNPs were conducted by the Wald test implemented in PLINK (version 1.03) to obtain a t-statistic for each tested SNP.

Pathway-based GWA analysis in the U.S. whites

The main procedures of pathway-based GWA analysis [7] were briefly summarized as follows:

1. Generation of gene-phenotype association rank: For x SNPs mapped to gene G_i (i = 1,…, N where N is the total number of genes with genotype data available in our GWA study), let r_i denote the absolute value of highest SNP-phenotype association statistic. The r_i was also assigned to represent the statistic value of gene-phenotype association for gene G_i. A gene list L (r_1,r_2,…, r_N) was generated by sorting all r_i from the largest to the smallest. Mostly, SNPs were mapped to their closest genes. And in rare cases, if a SNP is located within shared regions of two overlapping genes, the SNP was mapped to both genes.

2. Calculation of *ES*: For given pathway/gene set S, composed of N_S genes, ES^S was used to reflect the overrepresentation of S at the top of the entire ranked gene list L. ES^S was determined based on a weighted Kolmogorov-Smirnov like running-sum statistic:

$$ES^S = \max_{1\le i\le N}\left\{\sum_{G_{i^*}\in S, i^*\le i}\frac{|r_{i^*}|}{N_R} - \sum_{G_{i^*}\notin S, i^*\le i}\frac{1}{N-N_S}\right\}, \quad (1)$$

where $N_R = \sum_{G_{j^*}\in S}|r_{i^*}|$. From Formula (1), it is clear that ES^S is calculated by walking down the list L, increasing a running-sum statistic when we encounter a gene in S and decreasing it when we encounter genes not in S. The magnitude of the increment depends on the correlation of the gene with the phenotype. In short, ES^S is the maximum deviation from zero encountered in the random walk. It will be high if the association signal is concentrated at the top of list L, reflected by the significance level of observed ES^S (i.e. nominal p value).

3. Permutation and nominal significance assessment: The phenotype data was shuffled and permutation (*per)* was done to compute a ES^S_{per} through repeating steps (1) ~ (2) to estimate the nominal p value. A total of 1,000 permutations were done to create a histogram of the corresponding enrichment scores $ES^S_{per,null}$ for the given pathway/gene set S. The nominal p value was estimated as the percentage of permutations whose ES^S_{per} were greater than the observed ES^S.

4. Multiple testing adjustments: In order to correct the effects of gene size, for each pathway/gene set S, we calculated the normalized ES^S in the observed data and the normalized ES^S_{per} (NES^S_{per}) in all permutations. The calculation of normalized ES^S ($NES^{S)}$ relied on $ES^{S,}$ mean and standard deviation (SD) of ES^S_{per} in all permutations for the given pathway/gene set S*:*

$$NES^S = \frac{ES^S - mean(ES^S_{per})}{SD(ES^S_{per})}. \quad (2)$$

Then, in the context of multiple testing, *FWER p* value (denoted as p_{FWER}) was calculated through a highly conservative procedure, which sought to ensure that the reported results did not include even a single false positive gene set [7;20]. The p_{FWER} can be calculated as the fraction of all gene sets whose greatest NES^S_{per} in all permutations was higher than the NES^S in the given pathway/gene set S.

Validation analyses in Framingham samples

For a certain interesting pathway, we performed multiple step-wise regressions using SAS 8.2 (SAS Institute Inc., Cary, NC), to verify the associations of pathway genes with FN Z in Framingham samples, while adjusting for significant covariates ($p < 0.05$). At first, raw bone geometry value was adjusted through the same procedure, described above, for the U.S. whites. Then, association analyses for all the SNPs in certain interesting pathway were performed using the PLINK software package (version 1.02). In the multiple step-wise regression analysis, each pathway gene was represented by its top significant SNP as independent variable. *P* value of 0.05 was set as the criteria for the entry and removal of predictive variables. F test was used to assess the significance of the overall model. R-square value as an indicator of how well the model fits the data (e.g., an R-square close to 1.0 indicates that we have accounted for almost all of the variability with the variables specified in the model) was used to evaluate the additive contributions of pathway genes to the trait.

Other analyses

For our U.S. White sample, pathway-based GWA analyses were also conducted for FN BMD in the total population and for FN Z in the sex-specific groups through the same procedure described in the above sub-sections of "Routine statistical analysis" and "Pathway-based GWA analysis in the U.S. whites". In addition, to detect potential population stratification, which may lead to spurious association results, we used the software Structure 2.2 (http://pritch.bsd.uchicago.edu/software.html) to investigate the potential substructures of the U.S. whites sample and the Framingham sample. The program uses a Markov chain Monte Carlo (MCMC) algorithm to cluster individuals into different cryptic sub-populations on the basis of multi-locus genotype data [21]. To ensure the robustness of our results, we performed independent analyses under three assumed numbers for population strata (k = 2, 3, and 4), using 200 un-linked markers that were randomly selected across the entire genome. To confirm the results achieved through Structure 2.2, we further calculated inflation factors based on median chi-square statistic using a method of genomic control [22].

RESULTS

Pathway-based association analysis

In the pathway-based association analysis for FN Z in the total U.S. whites, 76 out of the 963 tested pathways showed significant association at the nominal significance level (p value < 0.05). Among them, two pathways were significant with p_{FWER} less than 0.05. One was 1- and 2-Methylnaphthalene degradation pathway retrieved from KEGG database (p_{FWER} value = 0.021) and the other was EphrinA-Eph receptors (EphR) signaling pathway queried from Ambion database (p_{FWER} value = 0.035) (Figure 1). For the other three tested bone geometric measures (CSA, CT and BR), no significant result was found after multiple testing adjustments, consequently, no further analyses were done for them.

In the sex-specific pathway-based GWA analysis for FN Z, we found the EphrinA-EphR pathway was significant in the male subgroup with a nominal p value of 0.006, while the 1- and 2-Methylnaphthalene degradation pathway was associated with FN Z in the female subgroup at a level of marginal significance (nominal p value = 0.056). However, these two correlations did not remain significant after adjusting for multiple tests. Furthermore, pathway-based GWA analysis showed that these two pathways were not associated with FN BMD (data not shown). In Table 2, basic information about the top 18 pathways associated with $-\lg(p)$ value > 2 in the pathway-based GWA analysis for FN Z in the total U.S. whites are summarized, including source database, database entry, pathway name, and association results in the total population as well as in the sex-specific groups.

1- and 2-Methylnaphthalene degradation pathway and EphrinA-EphR pathway are composed of 25 genes and 40 genes, respectively. Most of their pathway genes are covered by our genotype platform. Tables 3 and 4 individually list the information of SNPs representing the 21 1- and 2-Methylnaphthalene degradation pathway genes, and the 35 EphrinA-EphR pathway genes. A total of 15 genes in the 1- and 2-Methylnaphthalene degradation pathway and 21 genes in the EphrinA-EphR pathway were associated with FN Z at the nominal significance level (p value < 0.05). The most significant SNP in PAK gene, rs2105803, achieved a p value of 0.001 for FN Z. Figure 2 depicts running-sum plots for the two pathways ("Gene list rank" versus "ES^s") and a plot for –lg(p)values of all the 14,585 pathway genes ("Gene list rank" versus "-lg nominal p value") to describe the results of pathway-based GWA analysis for FN Z in the total U.S. whites sample. We observed that most of these two pathway genes were ranked at the top significance level among the 14,585 gene lists. Accordingly, the 1- and 2-Methylnaphthalene degradation pathway and EphrinA-EphR pathway achieved high *ESs* of 0.542 and 0.482, respectively.

Multiple step-wise regression analysis in Framingham samples

To validate our findings, we conducted multiple step-wise regression analyses for 1- and 2-Methylnaphthalene degradation pathway and EphrinA-EphR pathway in Framingham samples. After adjustment for age, age^2, sex, height and weight, 2 main-effect genes (ADH6 and ADH1A) were chosen out of 21 1- and 2-Methylnaphthalene degradation pathway genes (p value < 0.05). They composed the final model that had an overall p value of 0.0021 and could explain 1.24% of FN Z variation. While 8 main-effect genes (EphA1-2, EphA7-8, EFNA3, PAK1, PIK3CG and LIMK2) were chosen out of the 35 EphrinA-EphR pathway genes as predictive variables (p value < 0.05). They composed the final model that had an overall p value < 0.0001 and could explain 6.06% of FN Z variation.

Potential population stratification analyses

With 200 randomly selected unlinked SNPs, all the subjects in the U.S. whites sample were consistently clustered together under all the three assumed number of population strata, so were the subjects in the Framingham sample. Moreover, the inflation factors were estimated to be 1.030 (BR), 1.009 (Z), 1.035 (CSA) and 1.071 (CT) for U.S. whites sample, and 1.022 (BR), 1.013 (Z), 1.018 (CSA) and 1.047 (CT) for the Framingham sample, suggesting no significant population substructure in the two samples.

DISCUSSION

In this study, we used the genomic-wide based pathway approach to explore the joint effects of different gene variants in common pathways on FN bone geometry variations. Two pathways were identified as the most statistical promising pathways for FN Z after multiple testing adjustments, 1- and 2-Methylnaphthalene degradation pathway and EphrinA-EphR signaling cascade.

As we known, 1- and 2-Methylnaphthalene are components of polycyclic aromatic hydrocarbons (PAHs) present in cigarette smoke. A recent *in vivo* study showed PAHs may function as ligand for aryl-hydrocarbon receptor (AhR) a transcription factor that regulates gene expression, to cause the loss of bone mass and strength [23]. However, there has been little direct research into the effects of methylnaphthalene and its metabolites on bone and no biological correlation has been made thereof. In the present study, validation analysis in the Framingham sample demonstrated a significant but modest effect of 1- and 2-Methylnaphthalene degradation pathway genes (R-square=1.24%).

EphR and their cell-surface-bound ephrin ligands, including A- and B-subclass, constitute the largest subfamily of receptor protein-tyrosine kinases. EphrinA can activate EphA receptors and their downstream molecules (as reviewed in [24]). EphrinA-EphR pathway is known to function in reorganization of the actin cytoskeleton through Rho family GTPases. Rho family GTPases, including RhoA, Rac1 and Cdc42, have been implicated in the contraction of actin cytoskeletal systems, promoting the formation and elongation of lamellipodia and filopodia, respectively [25]. Since actin cytoskeleton including lamellipodia and filopodia are involved in the biological processes of osteoblastic adhesion and migration that are closely related to the bone geometry qualities, it is reasonable to hypothesize that EphrinA-EphR pathway may contribute to the genetic architecture underlying the variation of bone geometry.

In addition, the potential role of EphrinA-EphR pathway was revealed in the skeletal patterning (as reviewed in [26]). Several molecules such as ephrin A5 and EphA2-5 were expressed on the surface of osteoblasts or pre-osteoblasts [27–29]. Besides, the functions of EFNB2 in osteoclasts and EphB4 in osteoblasts were found to associate with the switch from bone resorption to bone formation [30]. In previous studies, crosstalks were detected between EFNB2 with both EphA3 and EphA4 [31–33], and between EphB2 and ephrinA5 [34]. These cross-talks may bridge A- and B-subclass Eph receptors/ephrins signaling, which suggested more complex regulation of EphrinA-EphR pathway in normal and pathological bone remodeling.

In this study, the pathway-based association analysis in U.S. whites demonstrated that 21 genes in this pathway were associated with FN Z at the nominal significance level (p value < 0.05). These genes included an ephrin (EPNA5) gene and 5 EphR genes (EphA1, EphA3-5 and EphA7), 2 Rho family member genes (Rac1 and cdc42) and their downstream p21-activated kinase genes (PAK1 and PAK7), 4 RhoA downstream genes (ROCK2, LIMK2, CFL1 and ACTG2), 3 adaptor molecular of EphR genes (PIK3CG, FAK1 and PTPN11), and others. Some of the identified pathway genes have been known to be important for bone, especially for osteoblasts. For example, RhoA-ROCK cascade was found to mediate the differentiation of human mesenchymal stem cells (hMSCs) to osteoblast and then promote osteogenesis, specifically via its effects on cytoskeletal tension [35]. GTPases Cdc42 and Rac were also suggested to communicate with receptor of advanced glycation end products to regulate the osteoblast motility [36]. PIK3CG, as an important modulator of extracellular signals, was found to be important for osteoblastic differentiation, recruitment, migration and survival [37–40]. In addition, activated EphA receptors can transmit signals to focal adhesion kinase (FAK), which is protein tyrosine kinase acting as a regulator of the integrin signaling cascade. This kinase was found to be important for mechanotransduction in osteoblasts [41]. Subsequent validation study confirmed our findings were by demonstrating the significant genetic effects of the same EphrinA-EphR pathway genes (EphA7, PAK1, PIK3CG and LIMK2) and the whole pathway on FN Z in the Framingham sample (Table 5).

On the whole, the evidences from multiple aspects (pathway-base GWA analyses, validation analyses and functional relevance to bone) strongly supported the importance of EphrinA-EphR pathway for FN Z. Nevertheless, this pathway was associated with FN Z but not with either the other three FN bone geometry parameters or FN BMD in the total U.S. whites. Besides, in the sex-stratified analysis, this pathway was shown to be associated with FN Z only in the male subgroup at a nominal significance level. These results may reflect site-specific effect due to genetic heterogeneity at different skeletal sites and sex-specific effect only present in male subjects. On the other hand, they might also be treated with caution because of the inflated false-positive and/or false-negative rates caused by increased multiple comparisons and insufficient power in individual subgroups. In this study, efforts like permutation-based adjustments have been taken to alleviate it.

Notably, no one EphrinA-EphR pathway gene attained GWA significance (4.2×10^{-7}) in our conventional GWA studies on FN bone geometry [42]. That is, pathway-based GWA approach may incorporate information from markers with moderate significance levels so as to detect novel genetic risk factors, which can serve as candidates for further replication studies. This approach has the merit of high-throughput in comparison with traditional candidate pathway association strategy, which may only figure out a very small fraction of the whole genetic architecture of complex diseases/traits. Besides, this approach provides an opportunity to systematically study a large number of pathways without assumptions about the causal pathways, and thus may have the higher power to identify new candidate genetic factors. However, a potential limitation of this study is that some of pathway genes were not covered by our genotype platform. For example, the genome coverage for EphrinA-EphR pathway was only 87.5%.

In summary, our results suggested that the polymorphisms in EphrinA-EphR pathway genes may affect FN bone geometry variations. Future molecular studies as well as validation studies with customized pathway array are necessary to further investigate this pathway in order to clarify its role in bone biology.

Acknowledgments

Investigators of this work were partially supported by grants from NIH (R01 AR050496, R21 AG027110, R01 AG026564, P50 AR055081 and R21 AA015973). The study also benefited from grants from National Science Foundation of China, Xi'an Jiaotong University, and the Ministry of Education of China. We also thank all contributors to the Framingham Heart Study. The Framingham Heart Study and the Framingham SHARe project are conducted and supported by the National Heart, Lung, and Blood Institute (NHLBI) in collaboration with Boston University. The Framingham SHARe data used for the analyses described in this manuscript were obtained through dbGaP. This manuscript was not prepared in collaboration with investigators of the Framingham Heart Study and does not necessarily reflect the opinions or views of the Framingham Heart Study, Boston University, or the NHLBI.

Abbreviations

PAK1	p21-activated kinase 1
FAK1	PTK2 protein tyrosine kinase 2
EphA7	Eph receptor A7
PIK3CG	phosphoinositide-3-kinase, catalytic, gamma
PAK7	p21-activated kinase 7
RASA1	RAS p21 protein activator 1
FYN	FYN oncogene related to SRC, FGR, YES
RAC1	ras-related C3 botulinum toxin substrate 1
EFNA5	ephrinA5
CDC42	cell division cycle 42
PTPN11	protein tyrosine phosphatase, non-receptor type 11
EphA3	Eph receptor A3
EphA1	Eph receptor A1
EphA5	Eph receptor A5
EphA4	Eph receptor A4
LIMK2	LIM domain kinase 2

ROCK2	Rho-associated, coiled-coil containing protein kinase 2
ADAM10	ADAM metallopeptidase domain 10
CFL1	cofilin 1 (non-muscle)
ACTG2	actin, gamma 2, smooth muscle, enteric
EphA8	Eph receptor A8
ACTB	beta actin
NGEF	neuronal guanine nucleotide exchange factor
FAK2	PTK2B protein tyrosine kinase 2 beta
PAK2	p21-activated kinase 2
ACTA2	actin, alpha 2, smooth muscle, aorta
PAK6	p21-activated kinase 6
PAK4	p21-activated kinase 4
CFL2	cofilin 2 (muscle)
ACTG1	actin, gamma 1
LIMK1	LIM domain kinase 1
EphA2	Eph receptor A2
ROCK1	Rho-associated, coiled-coil containing protein kinase 1
EFNA3	ephrinA3
ACTA1	actin, alpha 1, skeletal muscle
EFNB2	ephrinB2
DHRS2	dehydrogenase/reductase (SDR family) member 2
MYST3	MYST histone acetyltransferase (monocytic leukemia) 3
MYST4	MYST histone acetyltransferase (monocytic leukemia) 4
ADH1C	alcohol dehydrogenase 1C (class I), gamma polypeptide
ADHFE1	alcohol dehydrogenase, iron containing, 1
DHRS3	dehydrogenase/reductase (SDR family) member 3
ADH7	alcohol dehydrogenase 7 (class IV), mu or sigma polypeptide
LYCAT	lysocardiolipin acyltransferase 1
NAT5	N-acetyltransferase 5 (GCN5-related, putative)
SH3GLB1	SH3-domain GRB2-like endophilin B1
PNPLA3	patatin-like phospholipase domain containing 3
ADH4	alcohol dehydrogenase 4 (class II), pi polypeptide
ACAD8	acyl-Coenzyme A dehydrogenase family, member 8
ADH5	alcohol dehydrogenase 5 (class III), chi polypeptide
ADH6	alcohol dehydrogenase 6 (class V)
DHRS1	dehydrogenase/reductase (SDR family) member 1

ADH1A	alcohol dehydrogenase 1A (class I), alpha polypeptide
ESCO2	establishment of cohesion 1 homolog 2 (S. cerevisiae)
ESCO1	establishment of cohesion 1 homolog 1 (S. cerevisiae)
DHRS7	dehydrogenase/reductase (SDR family) member 7
ACAD9	acyl-Coenzyme A dehydrogenase family, member 9

References

1. Haleem S, Lutchman L, Mayahi R, Grice JE, Parker MJ. Mortality following hip fracture: trends and geographical variations over the last 40 years. Injury 2008;39:1157–63. [PubMed: 18653186]
2. Shen H, Long JR, Xiong DH, Liu YJ, Liu YZ, Xiao P, et al. Mapping quantitative trait loci for cross-sectional geometry at the femoral neck. J Bone Miner Res 2005;20:1973–82. [PubMed: 16234971]
3. Slemenda CW, Turner CH, Peacock M, Christian JC, Sorbel J, Hui SL, et al. The genetics of proximal femur geometry, distribution of bone mass and bone mineral density. Osteoporos Int 1996;6:178–82. [PubMed: 8704359]
4. Xiong DH, Shen H, Xiao P, Guo YF, Long JR, Zhao LJ, et al. Genome-wide scan identified QTLs underlying femoral neck cross-sectional geometry that are novel studied risk factors of osteoporosis. J Bone Miner Res 2006;21:424–37. [PubMed: 16491291]
5. Rivadeneira F, van Meurs JB, Kant J, Zillikens MC, Stolk L, Beck TJ, et al. Estrogen receptor beta (ESR2) polymorphisms in interaction with estrogen receptor alpha (ESR1) and insulin-like growth factor I (IGF1) variants influence the risk of fracture in postmenopausal women. J Bone Miner Res 2006;21:1443–56. [PubMed: 16939403]
6. Demissie S, Dupuis J, Cupples LA, Beck TJ, Kiel DP, Karasik D. Proximal hip geometry is linked to several chromosomal regions: genome-wide linkage results from the Framingham Osteoporosis Study. Bone 2007;40:743–50. [PubMed: 17079199]
7. Wang K, Li M, Bucan M. Pathway-Based Approaches for Analysis of Genomewide Association Studies. Am J Hum Genet 2007;81:1278–83.
8. Liu XG, Tan LJ, Lei SF, Liu YJ, Shen H, Wang L, et al. Genome-wide association and replication studies identified TRHR as an important gene for lean body mass. Am J Hum Genet 2009;84:418–23. [PubMed: 19268274]
9. Duan Y, Beck TJ, Wang XF, Seeman E. Structural and biomechanical basis of sexual dimorphism in femoral neck fragility has its origins in growth and aging. J Bone Miner Res 2003;18:1766–74. [PubMed: 14584886]
10. Rivadeneira F, Houwing-Duistermaat JJ, Beck TJ, Janssen JA, Hofman A, Pols HA, et al. The influence of an insulin-like growth factor I gene promoter polymorphism on hip bone geometry and the risk of nonvertebral fracture in the elderly: the Rotterdam Study. J Bone Miner Res 2004;19:1280–90. [PubMed: 15231015]
11. Beck T. Measuring the structural strength of bones with dual-energy X-ray absorptiometry: principles, technical limitations, and future possibilities. Osteoporos Int 2003;14 (Suppl 5):S81–8. [PubMed: 14504711]
12. Cupples LA, Arruda HT, Benjamin EJ, D'Agostino RB Sr, Demissie S, DeStefano AL, et al. The Framingham Heart Study 100K SNP genome-wide association study resource: overview of 17 phenotype working group reports. BMC Med Genet 2007;8 (Suppl 1):S1. [PubMed: 17903291]
13. Khoo BC, Beck TJ, Qiao QH, Parakh P, Semanick L, Prince RL, et al. In vivo short-term precision of hip structure analysis variables in comparison with bone mineral density using paired dual-energy X-ray absorptiometry scans from multi-center clinical trials. Bone 2005;37:112–21. [PubMed: 15869917]
14. Martin RB, Burr DB. Non-invasive measurement of long bone cross-sectional moment of inertia by photon absorptiometry. J Biomech 1984;17:195–201. [PubMed: 6736056]

15. Karasik D, Zhou Y, Cupples LA, Hannan MT, Kiel DP, Demissie S. Bivariate genome-wide linkage analysis of femoral bone traits and leg lean mass: Framingham study. J Bone Miner Res 2009;24:710–8. [PubMed: 19063671]
16. Ahn SJ, Costa J, Emanuel JR. PicoGreen quantitation of DNA: effective evaluation of samples pre- or post-PCR. Nucleic Acids Res 1996;24:2623–5. [PubMed: 8692708]
17. Singer VL, Jones LJ, Yue ST, Haugland RP. Characterization of PicoGreen reagent and development of a fluorescence-based solution assay for double-stranded DNA quantitation. Anal Biochem 1997;249:228–38. [PubMed: 9212875]
18. Di X, Matsuzaki H, Webster TA, Hubbell E, Liu G, Dong S, et al. Dynamic model based algorithms for screening and genotyping over 100 K SNPs on oligonucleotide microarrays. Bioinformatics 2005;21:1958–963. [PubMed: 15657097]
19. Rabbee N, Speed TP. A genotype calling algorithm for affymetrix SNP arrays. Bioinformatics 2006;22:7–12. [PubMed: 16267090]
20. Subramanian A, Tamayo P, Mootha VK, Mukherjee S, Ebert BL, Gillette MA, et al. Gene set enrichment analysis: a knowledge-based approach for interpreting genome-wide expression profiles. Proc Natl Acad Sci U S A 2005;102:15545–50. [PubMed: 16199517]
21. Pritchard JK, Stephens M, Donnelly P. Inference of population structure using multilocus genotype data. Genetics 2000;155:945–59. [PubMed: 10835412]
22. Devlin B, Roeder K. Genomic control for association studies. Biometrics 1999;55:997–1004. [PubMed: 11315092]
23. Lee LL, Lee JS, Waldman SD, Casper RF, Grynpas MD. Polycyclic aromatic hydrocarbons present in cigarette smoke cause bone loss in an ovariectomized rat model. Bone 2002;30:917–23. [PubMed: 12052463]
24. Lackmann M, Boyd AW. Eph, a protein family coming of age: more confusion, insight, or complexity? Sci Signal 2008;1:re2. [PubMed: 18413883]
25. Hall A. Rho GTPases and the actin cytoskeleton. Science 1998;279:509–14. [PubMed: 9438836]
26. Edwards CM, Mundy GR. Eph receptors and ephrin signaling pathways: a role in bone homeostasis. Int J Med Sci 2008;5:263–72. [PubMed: 18797510]
27. Allan EH, Hausler KD, Wei T, Gooi JH, Quinn JM, Crimeen-Irwin B, et al. EphrinB2 regulation by PTH and PTHrP revealed by molecular profiling in differentiating osteoblasts. J Bone Miner Res 2008;23:1170–81. [PubMed: 18627264]
28. Tanabe S, Sato Y, Suzuki T, Suzuki K, Nagao T, Yamaguchi T. Gene expression profiling of human mesenchymal stem cells for identification of novel markers in early- and late-stage cell culture. J Biochem 2008;144:399–408. [PubMed: 18550633]
29. Martin-Rendon E, Hale SJ, Ryan D, Baban D, Forde SP, Roubelakis M, et al. Transcriptional profiling of human cord blood CD133+ and cultured bone marrow mesenchymal stem cells in response to hypoxia. Stem Cells 2007;25:1003–12. [PubMed: 17185612]
30. Zhao C, Irie N, Takada Y, Shimoda K, Miyamoto T, Nishiwaki T, et al. Bidirectional ephrinB2-EphB4 signaling controls bone homeostasis. Cell Metab 2006;4:111–21. [PubMed: 16890539]
31. Lackmann M, Mann RJ, Kravets L, Smith FM, Bucci TA, Maxwell KF, et al. Ligand for EPH-related kinase (LERK) 7 is the preferred high affinity ligand for the HEK receptor. J Biol Chem 1997;272:16521–30. [PubMed: 9195962]
32. Cerretti DP, Vanden BT, Nelson N, Kozlosky CJ, Reddy P, Maraskovsky E, et al. Isolation of LERK-5: a ligand of the eph-related receptor tyrosine kinases. Mol Immunol 1995;32:1197–205. [PubMed: 8559144]
33. Kullander K, Klein R. Mechanisms and functions of Eph and ephrin signalling. Nat Rev Mol Cell Biol 2002;3:475–86. [PubMed: 12094214]
34. Himanen JP, Chumley MJ, Lackmann M, Li C, Barton WA, Jeffrey PD, et al. Repelling class discrimination: ephrin-A5 binds to and activates EphB2 receptor signaling. Nat Neurosci 2004;7:501–9. [PubMed: 15107857]
35. McBeath R, Pirone DM, Nelson CM, Bhadriraju K, Chen CS. Cell shape, cytoskeletal tension, and RhoA regulate stem cell lineage commitment. Dev Cell 2004;6:483–95. [PubMed: 15068789]

36. Rauvala H, Huttunen HJ, Fages C, Kaksonen M, Kinnunen T, Imai S, et al. Heparin-binding proteins HB-GAM (pleiotrophin) and amphoterin in the regulation of cell motility. Matrix Biol 2000;19:377–87. [PubMed: 10980414]

37. Fujita T, Azuma Y, Fukuyama R, Hattori Y, Yoshida C, Koida M, et al. Runx2 induces osteoblast and chondrocyte differentiation and enhances their migration by coupling with PI3K-Akt signaling. J Cell Biol 2004;166:85–95. [PubMed: 15226309]

38. Lee SU, Shin HK, Min YK, Kim SH. Emodin accelerates osteoblast differentiation through phosphatidylinositol 3-kinase activation and bone morphogenetic protein-2 gene expression. Int Immunopharmacol 2008;8:741–7. [PubMed: 18387517]

39. Nakasaki M, Yoshioka K, Miyamoto Y, Sasaki T, Yoshikawa H, Itoh K. IGF-I secreted by osteoblasts acts as a potent chemotactic factor for osteoblasts. Bone 2008;43:869–79. [PubMed: 18718566]

40. Zhang X, Zanello LP. Vitamin D receptor-dependent 1 alpha,25(OH)2 vitamin D3-induced anti-apoptotic PI3K/AKT signaling in osteoblasts. J Bone Miner Res 2008;23:1238–48. [PubMed: 18410228]

41. Young SR, Gerard-O'Riley R, Kim JB, Pavalko FM. Focal Adhesion Kinase is Important for Fluid Shear Stress Induced Mechanotransduction in Osteoblasts. J Bone Miner Res 2009;24:411–24. [PubMed: 19016591]

42. Zhao LJ, Liu XG, Liu YZ, Liu YJ, Papasian Christopher J, Shao BY, et al. Genome-wide association study for femoral neck bone geometry. J Bone Miner R Posted. online 13 Jul 2009.

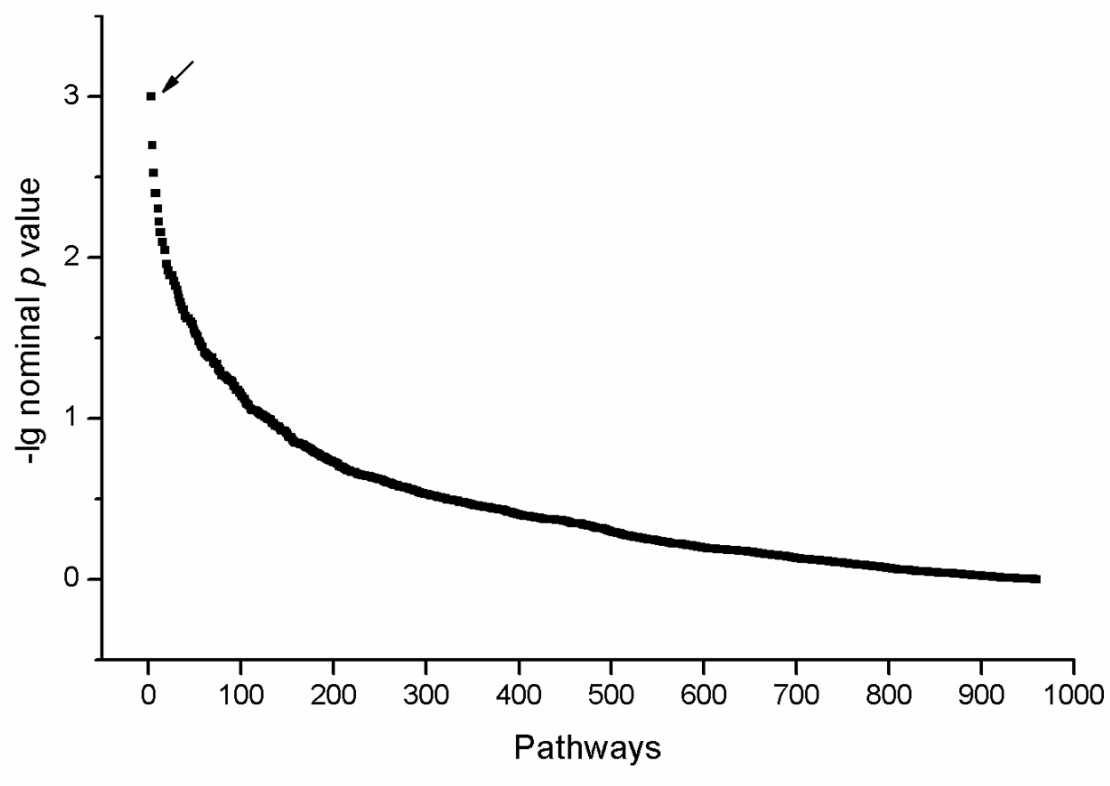

Figure 1.
Pathway-based genome-wide association results for FN Z in the total U.S. whites Note: Arrow points to the pathways associated with nominal *p* value < 0.001, including the 1- and 2-Methylnaphthalene degradation pathway and the EphrinA-EphR pathway.

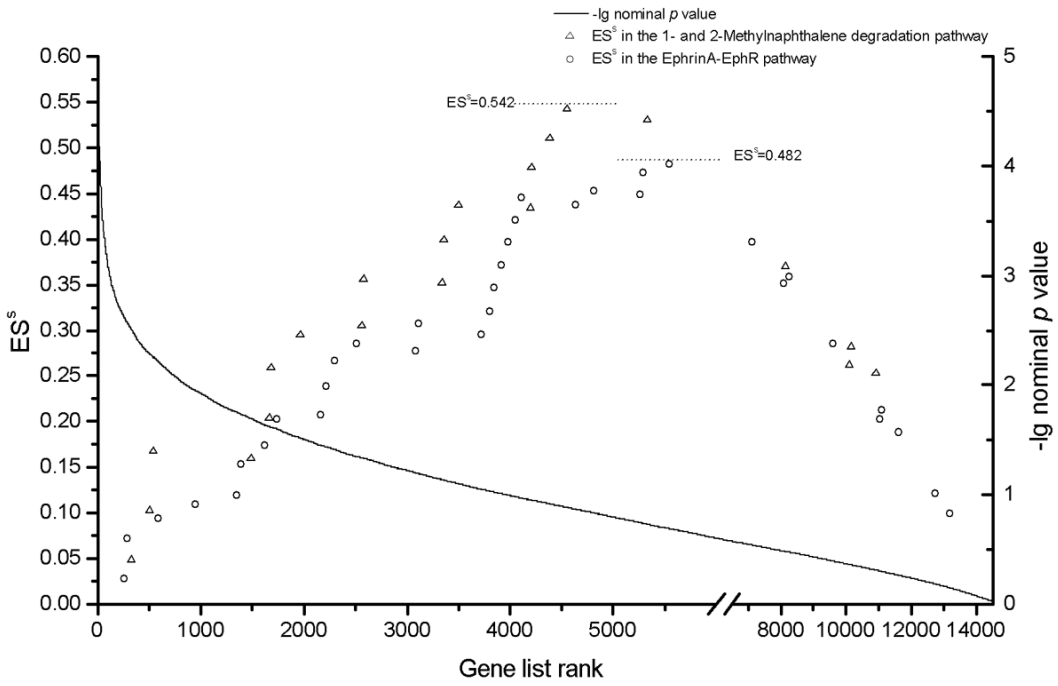

Figure 2.

Association results for the whole 14,585 genes and observed ES^S values for 1- and 2-Methylnaphthalene degradation pathway and EphrinA-EphR pathway genes Note: Gene list rank: rank in association significance in the whole gene list.

Table 1

Basic characteristics of the subjects

	U.S. whites		Framingham sample	
Trait	**Male (n = 501)**	**Female (n = 496)**	**Male (n = 469)**	**Female (n = 679)**
Age (years)	50.31 (18.87)	50.20 (17.70)	68.79 (9.91)	68.54 (11.58)
Height (m)	1.78 (0.07)	1.64 (0.07)	1.73 (0.07)	1.59 (0.07)
Weight (kg)	89.02 (14.94)	71.28 (15.92)	84.60 (15.28)	67.72 (14.01)
Z (cm^3)	2.27 (0.54)	1.49 (0.31)	1.82 (0.44)	1.24 (0.39)
CSA (cm^2)	3.20 (0.60)	2.48 (0.45)	2.70 (0.47)	2.09 (0.48)
CT (cm)	0.16 (0.03)	0.15 (0.03)	0.14 (0.02)	0.12 (0.03)
BR	12.42 (2.69)	11.61 (2.74)	15.38 (3.60)	15.09 (4.28)

Note: Data presented are unadjusted means (SD).

Table 2

Basic information for the top 18 pathways in the pathway-based GWA analysis for FN Z in the total U.S. whites

Entry	Pathway name	Source	Total	Male	Female
Hsa00624	1- and 2-Methylnaphthalene degradation	KEGG	< 0.001	-	0.056
Amb121	EphrinA-EphR Signaling	Ambion	< 0.001	0.006	-
GO:0051051	Negative regulation of transport	GO	< 0.001	-	-
Hsa01031	Glycan structures - biosynthesis 2	KEGG	0.002	0.035	-
StemPathway	Regulation of hematopoiesis by cytokines	BioCarta	0.003	-	-
cdc42racPathway	Role of PI3K subunit p85 in regulation of Actin Organization and Cell Migration	BioCarta	0.003	0.011	-
GO:0030097	Hemopoiesis	GO	0.004	-	0.081
Hsa00960	Alkaloid biosynthesis II	KEGG	0.004	0.002	-
Hsa04810	Regulation of actin cytoskeleton	KEGG	0.004	-	-
GO:0016776	Phosphotransferase activity, phosphate group as acceptor	GO	0.005	-	-
Amb1	14-3-3 and Cell Cycle Regulation	Ambion	0.006	-	-
GO:0016616	Oxidoreductase activity, acting on the CH-OH group of donors, NAD or NADP as acceptor	GO	0.007	0.004	-
GO:0008285	Negative regulation of cell proliferation	GO	0.007	0.069	0.088
Amb285	PDGF Pathway	Ambion	0.007	0.053	-
Edg1Pathway	Phospholipids as signalling intermediaries	BioCarta	0.008	-	-
GO:0016799	Hydrolase activity, hydrolyzing N-glycosyl compounds	GO	0.008	0.004	-
Amb265	Oct4 in Mammalian ESC Pluripotency	Ambion	0.009	-	-
Hsa00350	Tyrosine metabolism	KEGG	0.009	0.061	-

Note: All: association results for FN Z in the total sample; Male, Female: association results for FN Z in the male and female subgroups, respectively. “-” denotes nominal *p* value > 0.01.

Table 3

Genes in the 1- and 2-Methylnaphthalene degradation pathway

Gene	Max_SNP	Allele	MAF	Chr	Phy_loc	Role	*p*_max_snp
DHRS2	rs12894928	G/T	0.46	14	23266975	Upstream	0.002
MYST3	rs13270574	C/T	0.44	8	42121063	Upstream	0.003
MYST4	rs11001246	C/T	0.05	10	76450308	Upstream	0.003
ADH1C	rs1229979	C/T	0.31	4	100474976	Upstream	0.011
ADHFE1	rs2465983	C/T	0.17	8	67526166	Downstream	0.012
DHRS3	rs4394668	C/T	0.21	1	12593816	Downstream	0.012
ADH7	rs1154436	C/T	0.29	4	100504374	Upstream	0.015
LYCAT	rs6742360	G/T	0.05	2	30639989	Upstream	0.021
NAT5	rs6081840	C/T	0.43	20	19956581	Upstream	0.022
SH3GLB1	rs12097397	C/G	0.05	1	86987942	Upstream	0.031
PNPLA3	rs16991187	A/C	0.10	22	42672731	Upstream	0.032
ADH4	rs17817958	G/T	0.30	4	100280268	Upstream	0.034
ACAD8	rs473041	A/G	0.34	11	133631822	Upstream	0.045
ADH5	rs2602891	C/T	0.30	4	100262307	Upstream	0.045
ADH6	rs6837311	A/T	0.39	4	100414296	Upstream	0.048
DHRS1	rs4568	A/G	0.25	14	23829849	Downstream	-
ADH1A	rs17583753	A/G	0.15	4	100404687	Upstream	-
ESCO2	rs17057863	C/T	0.09	8	27700791	Downstream	-
ESCO1	rs16942790	C/T	0.16	18	17369129	Downstream	-
DHRS7	rs425565	C/G	0.14	14	59673636	Downstream	-
ACAD9	rs789254	A/G	0.29	3	130057283	Downstream	-

Note: “Max_SNP”: the most significant SNP; “MAF”: minor allele frequency in our sample; “Chr”: chromosome; “Phy_loc”: physical location; “-” denotes that *p* value > 0.05.

Table 4

Genes in the EphrinA-EphR signaling pathway

Gene	Max_SNP	Allele	MAF	Chr	Phy_loc	Role	*p*_max_snp
PAK1	rs2105803	A/G	0.21	11q14.1	76911659	Upstream	0.001
FAK1	rs11167023	A/G	0.18	8q24.3	142175410	Upstream	0.002
EphA7	rs6941459	C/T	0.44	6q16.1	94593345	Upstream	0.003
PIK3CG	rs10953518	A/G	0.14	7q22.3	106187118	Upstream	0.006
PAK7	rs742452	C/G	0.23	20p12.2	9684363	Intron	0.009
RASA1	rs3827607	A/G	0.42	5q14.3	86712976	Intron	0.010
FYN	rs2182644	A/G	0.09	6q21	112245575	Intron	0.012
RAC1	rs836472	C/T	0.25	7p22.1	6401429	Intron	0.013
EFNA5	rs17159152	C/T	0.27	5q21.3	106206807	Downstream	0.017
CDC42	rs17837965	A/G	0.05	1p36.12	22267212	Intron	0.017
PTPN11	rs7132204	A/G	0.39	12q24.13	111688424	Downstream	0.018
EphA3	rs6797260	A/T	0.32	3p11.2	89385176	Intron	0.021
EphA1	rs7800937	A/G	0.08	7q35	142803429	Intron	0.028
EphA5	rs1514271	C/G	0.34	4q13.1	65799362	Downstream	0.028
EphA4	rs17349283	A/G	0.46	2q36.1	221798041	Downstream	0.037
LIMK2	rs2267171	C/T	0.07	22q12.2	29979632	Intron	0.038
ROCK2	rs6716817	A/G	0.47	2p25.1	11303285	Intron	0.039
ADAM10	rs4775085	A/G	0.06	15q22.1	56737283	Intron	0.040
CFL1	rs3903072	A/C	0.48	11q13.1	65339642	Downstream	0.042
ACTG2	rs1721241	C/G	0.22	2p13.1	73981899	Intron	0.043
EphA8	rs12128121	A/G	0.10	1p36.12	22804749	Downstream	0.044
ACTB	rs1474445	C/T	0.18	7p22.1	5563375	Upstream	-
NGEF	rs895432	C/T	0.05	2q37.1	233465941	Coding exon	-
FAK2	rs2251430	A/G	0.14	8p21.2	27364766	Intron	-
PAK2	rs843530	C/T	0.46	3q29	197965421	Intron	-
ACTA2	rs1937330	A/T	0.08	10q23.31	90844025	Upstream	-
PAK6	rs8035733	A/G	0.18	15q15.1	38330232	Intron	-
PAK4	rs513053	A/G	0.38	19q13.2	44332986	Intron	-
CFL2	rs17453240	C/G	0.09	14q13.2	34248919	3′ near gene	-

Gene	Max_SNP	Allele	MAF	Chr	Phy_loc	Role	*p*_max_snp
ACTG1	rs9907460	G/T	0.38	17q25.3	77066757	Downstream	-
LIMK1	rs2855726	A/G	0.33	7q11.23	73155050	Intron	-
EphA2	rs904107	A/G	0.05	1p36.13	16361410	Promoter	-
ROCK1	rs1552110	A/G	0.05	18q11.1	16924725	Intron	-
EFNA3	rs7368345	A/G	0.50	1q22	153346714	Downstream	-
ACTA1	rs499689	C/T	0.40	1q42.13	227632355	Downstream	-

Note: “Max_SNP”: the most significant SNP; “MAF”: minor allele frequency in our sample; “Chr”: chromosome; “Phy_loc”: physical location; “-” denotes that *p* value > 0.05.

Table 5

Results for the multiple step-wise regression analysis for EphrinA-EphR pathway in the Framingham sample

Intercept/Gene	Max_SNP	Parameter Estimate	Standard Error	*p* value
Intercept	**-**	**1.721**	**0.138**	**< 0.0001**
EphA1	rs12703526	−0.007	0.002	0.001
PIK3CG	rs6958639	−0.006	0.002	0.001
EphA2	rs4661717	0.026	0.009	0.006
EphA8	rs209693	−0.008	0.003	0.006
EphA7	rs6935730	0.006	0.002	0.011
LIMK2	rs2106294	0.004	0.002	0.021
PAK1	rs568309	0.004	0.002	0.024
EFNA3	rs7368345	0.005	0.002	0.033

Note: “Max_SNP” denotes the most significant SNP.